# Electrostatic Effects on Ion Selectivity and Rectification in Designed Ion Channel Peptides

**J. D. Lear,* J. P. Schneider, P. K. Kienker,† and W. F. DeGrado***

*Contribution from the Johnson Research Foundation, Department of Biochemistry & Biophysics, University of Pennsylvania, Philadelphia, Pennsylvania 19104-6059*

*Received August 23, 1996*[⊗]

**Abstract:** To help determine how amino acid sequence can influence ionic conduction properties in α-helical structures, we have synthesized and studied three closely related, channel-forming peptides. The sequences are based on a 21-residue amphiphilic Leu-Ser-Ser-Leu-Leu-Ser-Leu heptad repeat motif and differ in having either neutral, negatively, or positively charged N-termini. The channels formed by the neutral peptide are modestly cation selective and exhibit asymmetric current-voltage curves arising from the partial charges at the ends of the α-helix. Addition of a negatively charged Glu residue converted the channel to a completely cation-selective structure and essentially eliminated its rectification. Addition of a positively charged Arg residue near the N-terminus of the peptide reduced this channel's cation selectivity and increased the extent of rectification. These effects on channel ionic conductance can be explained by a theoretical electrostatic model and provide insights into the workings of more complex channel proteins.

Ligand-gated ion channels in the central nervous system have significant charge selectivity.[1] Excitatory ligand (e.g., acetylcholine, glutamate) receptor channels are very selective for positive ions and promote the generation of nerve impulses by allowing extracellular cations ($Na^+$, $Ca^{2+}$) to cross the postsynaptic membrane. Corresponding inhibitory ligand (e.g., γ-amino butyric acid, glycine) receptor channels counteract the depolarizing effects of positive ion flux by selectively allowing chloride ions to cross the membrane. Both classes of channels are important targets in medicinal chemistry, and their structure−property relationships are of great interest. However, the large size and extreme complexity of such ion channel proteins make it difficult to understand their mechanisms at the atomic level. This problem can be reduced somewhat by studying the properties of the pore-lining segments of natural ion channel proteins[2] or helix-forming antibiotic peptides.[3] However, even in these simplified systems, considerable complexity remains, making interpretation difficult. Thus, upon inspection of an ion channel sequence, it is currently not possible to predict *a priori* the contribution of a given amino acid residue to the conductance properties of the channel. Therefore, we have constructed a "minimalist" peptide (Ac-(LSSLLSL)$_3$; Ac = acetyl; C-terminus = $CONH_2$) that contains the simplest features consistent with formation of an amphiphilic, channel-forming α-helix.[4] After careful characterization of this peptide's channel-forming properties,[5] it is now possible to ask how the addition of a charged residue will affect its ion selectivity and rectification properties.

A wealth of information[6] suggests that Ac-(LSSLLSL)$_3$ associates into channels consisting of a bundle of approximately six parallel, transmembrane helices with apolar Leu residues (L) projecting toward the bilayer and polar Ser residues (S) lining the pore. The channels have a moderate degree of selectivity for cations relative to anions, presumably because of the orientation of the hydroxyl groups of the seryl side chains in the pore.[7] Although the channels formed by Ac-(LSSLLSL)$_3$ are formally neutral, α-helical peptides have partial charges of approximately +0.5 and −0.5 near their N- and C-termini, respectively, due to the alignment of their amide groups.[8] This asymmetric charge distribution strongly influences their channel-forming and ion-conduction properties. For instance, the frequency of formation of Ac-(LSSLLSL)$_3$ channels increases exponentially with the applied transmembrane voltage, which helps to unidirectionally orient the peptides in a transmembrane configuration conducive to forming a parallel helical bundle. In the absence of a transmembrane voltage, these peptides prefer to lie in the membrane with their helical axes parallel to the membrane surface. However, the applied voltage aligns a fraction of the helices in a unique transmembrane orientation. For instance, if the peptide is added to one side of the bilayer and the opposite side is held at positive potential, this will attract the partial negative charge of the C-terminal carboxamide, causing this end of the helix to cross the bilayer and assume a transmembrane orientation.

The electrostatic asymmetry of a parallel helical bundle can also account for the highly asymmetric, single channel current-voltage curves (rectification) observed for Ac-(LSSLLSL)$_3$. Current-voltage curves for this peptide are generally obtained by first applying a potential to orient the peptides in the bilayer and initiate channel formation. Once a single channel is observed, the voltage is rapidly (10 mV/ms) ramped from approximately −200 mV to +200 mV to allow the measurement of a current-voltage curve on a single channel. When the lifetime of a single channel is long enough, this technique allows current-voltage curves to be measured at both positive and

* Authors to whom correspondences should be addressed.
† Department of Physiology & Biophysics, Albert Einstein College of Medicine, Bronx, NY 10461.
⊗ Abstract published in *Advance ACS Abstracts,* March 15, 1997.
(1) Nicoll, R. A.; Malenka, R. C.; Kauer, J. A. *Physiol. Rev.* **1990**, *70*, 513−565.
(2) Montal, M. *Current Opin. Struct. Biol.* **1995**, *5*, 501−506.
(3) Sansom, M. S. P. *Prog. Biophys. Mol. Biol.* **1991**, *55*, 139−235.
(4) DeGrado, W. F.; Wasserman, Z. R.; Lear, J. D. *Science* **1989**, *243*, 622−628.
(5) Kienker, P. K.; Lear, J. D. *Biophys. J.* **1995**, *68*, 1347−1358.
(6) Åkerfeldt, K. S.; Kienker, P. K.; Lear, J. D.; DeGrado, W. F. In *Comprehensive Supramolecular Chemistry*; Reinhoudt, D. N., Ed.; Pergamon: London, 1996; Vol. 10, pp 659−686.
(7) Åkerfeldt, K. S.; Lear, J. D.; Wasserman, Z. R.; Chung, L. A.; DeGrado, W. F. *Acc. Chem. Res.* **1993**, *26*, 191−197.
(8) Hol, W. G. J. *Progr. Biophys. Mol. Biol.* **1985**, *45*, 149−195.

S0002-7863(96)02967-8 CCC: $14.00 

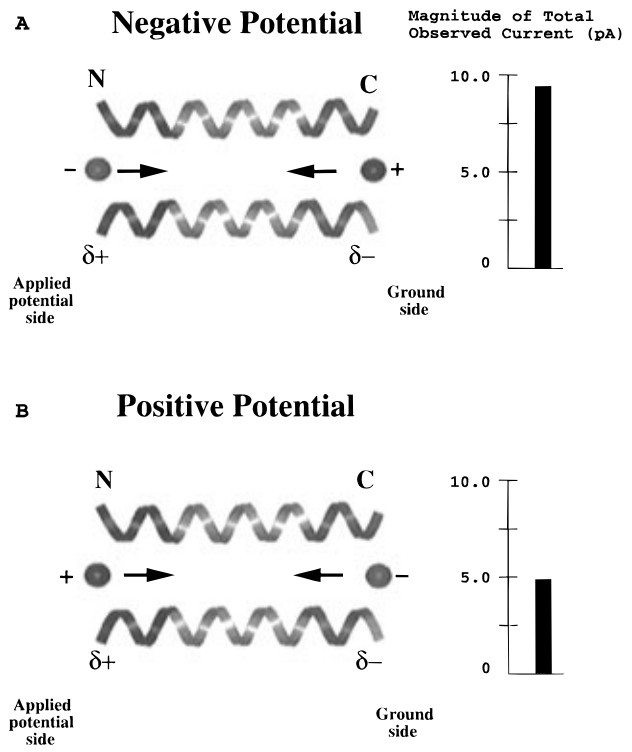


**Figure 1.** Schematic diagram of the conduction of ions through the Ac-(LSSLLSL)$_3$ channel. For clarity, only two helices of the proposed hexameric bundle are shown. $\delta^+$ and $\delta^-$ refer to the partial charges near the N- anc C-terminus of a formally neutral α-helix. The Ac-(LSSLLSL)$_3$ helices are preoriented in a parallel bundle with the C-terminus of each helix positioned on the zero (ground) potential side of the membrane by the preramp holding potential. (A) The current observed when the applied potential is negative is comprised of two distinct fluxes: the flow of cations from the channel C-terminus toward the N-terminal side and the flow of anions from the N-terminus toward the C-terminus. (B) When the applied voltage is changed quickly to positive, the direction of both ion fluxes is reversed with respect to the fixed channel orientation. The heights of the bars next to the schematic channels are proportional to the total current (the sum of the cation and anion fluxes) observed at ±100 mV for the Ac-(LSSLLSL)$_3$ peptide channels in 1 M KCl.

negative potentials on a channel with a defined orientation. Hundreds of channel openings are recorded and averaged to improve the signal-to-noise ratio. Figure 1 illustrates how the partial charges of the parallel helical bundle give rise to rectification. At the beginning of a recording, the Ac-(LSSLLSL)$_3$ helices are oriented with the N-terminus of each helix positioned on the negative potential side of the membrane. The overall current observed when the voltage is negative on the N-terminal side is comprised of the flow of anions from the channel N-terminus toward the C-terminal (ground potential) side and the flow of cations from the C-terminus toward the N-terminus. When the applied voltage is positive on the N-terminal side the ions flow in the reverse directions. The total current at positive potential is smaller than the current at negative potential because at positive potential both cations and anions must traverse an electrically repulsive vestibule as they enter the N- and C-terminal sides of the channel, respectively. Conversely, with an applied negative potential, both cations and anions experience an electrostatic attraction as they enter the channel at the C- and N-termini, respectively, so total current is increased. Thus, for a channel such as this, in which ion entry appears to be rate-determining, the electrostatic environment of the mouth of the channel can have a very large effect on conductance.

It is interesting that although the partial charges on the helices can account for the observed current rectification, they cannot account for the modest cation selectivity observed for Ac-(LSSLLSL)$_3$. This is because a parallel bundle of Ac-(LSSLLSL)$_3$ helices has equal-but-opposite partial charges on either side of the pore (Figure 1). As a result, the electrostatic potential associated with a cation entering from one end of the channel will always be equivalent to that experienced by an anion entering on the other (oppositely charged) end of the channel. Thus, the moderate charge selectivity observed for this peptide appears to be related to the lining of the pore rather than the partial charges at the ends of the α-helices.

In this paper we further test and extend this model by asking how the addition of a formally charged residue to just one end of the helix will affect the ion selectivity and rectification of the Ac-(LSSLLSL)$_3$ channel. To investigate this feature, two peptides of sequence Ac-EW-(LSSLLSL)$_3$ and Ac-RW-(LSSLLSL)$_3$ were prepared, and the conductance properties of their corresponding ion channels were characterized for comparison to those of the Ac-(LSSLLSL)$_3$ peptide. Addition of a negatively charged Glu (E) residue at the N-terminus should decrease the electrostatic asymmetry of the peptide, converting it to a structure with terminal charges of −0.5 at both ends of the helix (assuming the charge of the initial helix was 0.5 and −0.5 at the N- and C-termini, respectively). In contrast, addition of a positively charged Arg (R) at the N-terminus increases the overall electrostatic asymmetry, giving a peptide with an N-terminal charge of 1.5 and a C-terminal charge of −0.5. In each peptide, the charged residue lies on the polar, Ser-containing side of the α-helix, and the adjacent Trp (W) provides a convenient spectroscopic tag. As in Ac-(LSSLLSL)$_3$, the C-terminus was blocked with a formally neutral carboxamide to facilitate its insertion into bilayers for channel formation.[9]

The addition of a charged residue to just the N-terminus of the helix should have a large effect on *both* rectification and charge selectivity, because this change should affect the conductance of ions flowing from the N-terminal portion of the pore without significantly affecting conductance of ions from the other, uncharged end. For instance, the addition of a negative charge as in Ac-EW-(LSSLLSL)$_3$ would be expected to lead to an increase in cation-selectivity and a decrease in rectification; now the electrostatic environment at the entry of the channel should favor conductance of cations over anions irrespective of the side from which they enter (Figure 1). Also, the current-voltage asymmetry should be reduced in concert with the decrease in the electrostatic asymmetry of the peptide. By analogous reasoning, adding a positive charge to the N-terminus as in Ac-RW-(LSSLLSL)$_3$ should result in an increase of current-voltage curve asymmetry and a decrease in the cation selectivity.

## Results

**Peptides.** The peptides were prepared by segment condensation (Experimental Section), providing compounds that could

(9) The parallel helix bundle model for the Ac-(LSSLLSL)$_3$ peptide channels is based largely on the observed dependence of channel open probability on transmembrane voltage and on the sign of the voltage dependence relative to the helical dipole. The Ac-EW- peptide, with an ionized Glu side chain, appears to have no net dipole moment so we cannot infer the orientation from the sign of the applied potential alone. However, we have observed that peptides with a single N-terminally charged residue (including Ac-RW-(LSSLLSL)$_3$ and $H_2N$-(LSSLLSL)$_3$) appear to form channels by preferentially inserting their formally uncharged C-terminal carboxamide into the bilayer. We speculate that this is because insertion of the more polar charged group would have a much higher energetic barrier to overcome. Thus when these peptides are added to only one side of a pre-formed bilayer, channels are formed at significantly greater rates when the potential is positive on the side opposite to that of peptide addition (trans-positive) as opposed to a trans-negative potential. The trans-positive potential presumably attracts the partial negative charge of the peptide helix C-terminus. Similar data are observed for Ac-EW-(LSSLLSL)$_3$, suggesting that it also inserts its formally neutral C-terminus in preference to its N-terminus which contains the formally charged Glu residue.

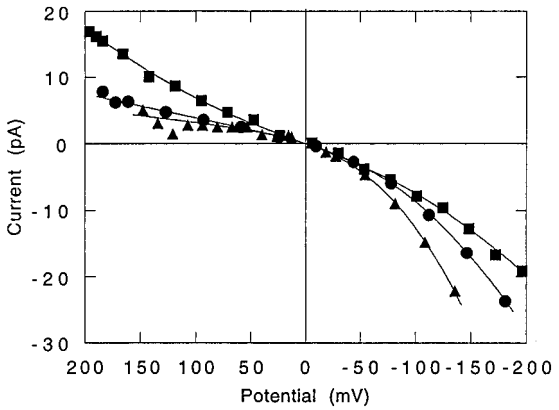


**Figure 2.** Current-voltage curves for Ac-(LSSLLSL)$_3$ (circles), Ac-EW-(LSSLLSL)$_3$ (squares), and Ac-RW-(LSSLLSL)$_3$ (triangles). The lines represent theoretical curves generated from eq 2 fit to the weighted data at ~1 mV intervals. Data points are shown at wider voltage intervals for clarity.

readily be purified to homogeneity. The Trp residue provides a convenient fluorescent tag for monitoring incorporation of the peptides into membranes and also to evaluate their position in the bilayer. An emission maximum of 332 nm was observed for Ac-EW-(LSSLLSL)$_3$, consistent with the value obtained from earlier work[10] on Trp-substituted derivatives of (LSSLLSL)$_3$ suggesting that Ac-EW-(LSSLLSL)$_3$ binds in an orientation analogous to (LSSLLSL)$_3$.

**Comparison of Ac-(LSSLLSL)$_3$, Ac-EW-(LSSLLSL)$_3$, and Ac-RW-(LSSLLSL)$_3$ Peptide Channels.** Each of these peptides in 1 M KCl, formed channels in planar bilayers with lifetimes sufficiently long to allow current-voltage curves to be measured on single channels. At 1 M salt concentration, the quality of the single channel recordings was similar to that previously described for Ac-(LSSLLSL)$_3$ .[6] At lower salt concentrations, it was difficult to measure single channel properties of the Ac-RW-(LSSLLSL)$_3$ channel, possibly because charge repulsion between the Arg side chains led to low channel lifetime or membrane disruption. In 1 M KCl, the mean lifetime of channels formed from Ac-(LSSLLSL)$_3$ is approximately 200 ms;[11] Ac-EW-(LSSLLSL)$_3$ has a shorter lifetime (~100 ms), and the lifetime of Ac-RW-(LSSLLSL)$_3$ is also shorter (~50 ms). The current-voltage curves for the neutral Ac-(LSSLLSL)$_3$, the negatively charged Ac-EW-(LSSLLSL)$_3$, and the positively charged Ac-RW-(LSSLLSL)$_3$ peptide channels show that the N-terminal charge indeed has a large influence on current-voltage curve asymmetry (Figure 2). The Ac-(LSSLLSL)$_3$ channel is about 2-fold more conductive at −125 mV than at +125 mV, indicative of its inherent electrostatic asymmetry as described above. Addition of an Arg to the N-terminus (Ac-RW-(LSSLLSL)$_3$) markedly increases the rectification; at −125 mV this channel is 4- to 6-fold more conductive than at +125 mV. On the other hand, addition of a negatively charged Glu to the N-terminus (Ac-EW-(LSSLLSL)$_3$) decreases the rectifying behavior; this channel is nearly as conductive at +125 mV as it is at −125 mV. Further, the degree of rectification for this peptide is pH-dependent. At pH 4.5, near the intrinsic p$K_a$ of the Glu carboxylate, the rectification falls to about half that observed at pH 9. At pH 2, it becomes the same as that observed for the Ac-(LSSLLSL)$_3$ channel.

These results are in excellent qualitative agreement with our model. In particular, the Ac-EW-(LSSLLSL)$_3$ channel shows an increase in total current at positive potential and a decrease at negative potential compared to the Ac-(LSSLLSL)$_3$ channel, attributable to parallel changes in the flux of cations and anions, respectively. Conversely, the Ac-RW-(LSSLLSL)$_3$ channel shows the opposite behavior as would be predicted from the qualitative model. A more quantitative analysis of the curves will be discussed below.

**Charge Selectivity.** The charge selectivity of an ion channel is generally evaluated by measuring its conductance with different concentrations of the same electrolyte on either side of the bilayer. In the absence of an applied potential, the ions tend to move through the channel down their concentration gradients. If the channel is nonselective (i.e., it does not kinetically discriminate between anions versus cations), no net current is observed in the absence of an applied potential, because the oppositely charged ions move through the channel at equal rates. On the other hand, if the channel shows charge selectivity, a net electrical conductance is observed. Conventionally, the selectivity is measured by determining the "reversal potential" ($E_{rev}$), which is the transmembrane electrical potential required to achieve zero current with a given asymmetric salt concentration. If the channel is nonselective the reversal potential is zero, whereas if the channel is perfectly selective the reversal potential will be equal to the difference in the chemical potential of the permeant ion on the two sides of the bilayer. More generally, the ionic selectivity of a channel is frequently defined by the ion permeability ratio (in this case, $P_K/P_{Cl}$) calculated by fitting reversal potentials to the Goldman−Hodgkin−Katz eq 1

$$\frac{P_K}{P_{Cl}} = \frac{[a_{Cl}]_V - [a_{Cl}]_0 \exp(FE_{rev}/RT)}{[a_K]_V \exp(FE_{rev}/RT) - [a_K]_0} \quad (1)$$

where the $a$'s denote thermodynamic activities on the applied potential (V) and ground (0) sides of the membrane, $F$ is Faraday's constant, and $RT$ is thermal energy.[12]

For Ac-EW-(LSSLLSL)$_3$ (Figure 3a), dilution of the KCl electrolyte on the ground side of the bilayer (corresponding to the C-terminal end of the channel;[9] Figure 1) reduces the current at negative potential and shifts the reversal potential toward more negative values. This is indicative of cation selectivity, as previously observed for the uncharged Ac-(LSSLLSL)$_3$ channel.[5] However, the degree of the shift with dilution (Figure 3c) is significantly greater for the Ac-EW-(LSSLLSL)$_3$ channel. The calculated value of the cation selectivity ($P_K/P_{Cl}$) for the Ac-EW-(LSSLLSL)$_3$ channel approaches infinity, indicative of a perfectly cation selective channel. By comparison, $P_K/P_{Cl}$ for the Ac-(LSSLLSL)$_3$ channel under these experimental conditions is approximately 10.

In contrast to the cation selectivity observed for the uncharged and negatively charged peptides, the Ac-RW-(LSSLLSL)$_3$ channel ($P_K/P_{Cl} = 1.1$) displays reduced currents at both positive and negative potentials upon dilution of the KCl on the C-terminal side of the channel (Figure 3b), and there is very little shift in the reversal potential (Figure 3c). Both of these features indicate that this channel conducts cations and anions about equally well over the range of conditions examined. Thus, the sign of the N-terminal charge can predictably modulate the modest intrinsic charge-selectivity of Ac-(LSSLLSL)$_3$ to make it either highly cation selective or non-selective. These changes are easily rationalized according to the model in Figure 1.

(10) Chung, L. A.; Lear, J. D.; DeGrado, W. F. *Biochemistry* **1992**, *31*, 6608−6616.
(11) Kienker, P. K.; DeGrado, W. F.; Lear, J. D. *Proc. Natl. Acad. Sci. U.S.A.* **1994**, *91*, 4859−4863.
(12) Hille, B. *Ionic Channels of Excitable Membranes*, 2nd ed.; Sinauer Associates, Inc.: Sunderland, MA, 1992.
(13) Parsegian, V. A. *Ann. N. Y. Acad. Sci.* **1975**, *264*, 161−174.
(14) The effect on the curve-fitting results of adding 3 Å to the channel length is small. For example, using $L = 30$ Å instead of $L = 33$ Å in fitting the Ac-EW-(LSSLLSL)$_3$ data increased the fitted value of $Z_n$ by only 4%.

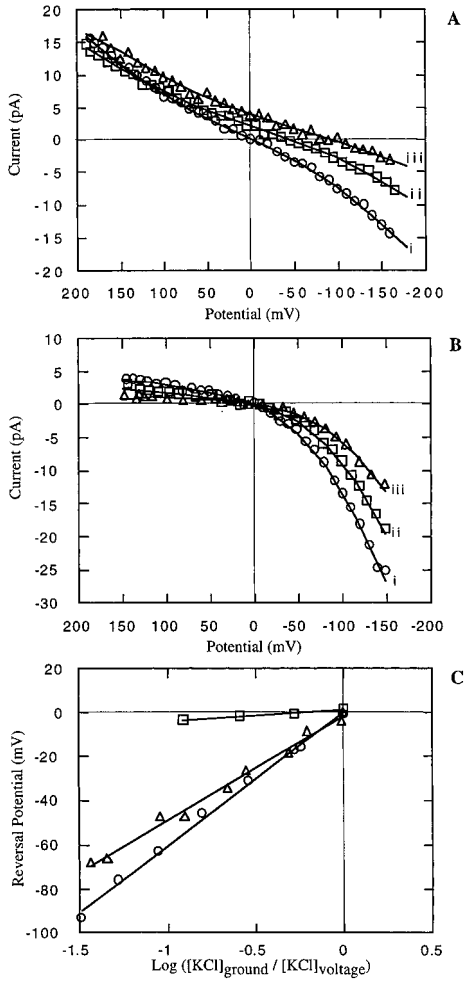


**Figure 3.** Representative current-voltage curves for asymmetric KCl concentrations for channels formed by (A) Ac-EW-(LSSLLSL)$_3$ and (B) Ac-RW-(LSSLLSL)$_3$. Successive dilutions were made of the initially symmetric 1 M KCl electrolyte on the zero (ground) holding potential side of the bilayer membrane using KCl-free buffer. The ratios of KCl activities (calculated from the measured solution conductivities and standard data tables) on the ground- vs the holding-potential side were (A) i = 1.00, ii = 0.289, iii = 0.0323 and (B) i = 1.00, ii = 0.53, iii = 0.122. Panel C shows reversal potentials, determined by fifth order polynomial interpolation of current-voltage data from experiments such as (and including) those in panels A and B and corrected for liquid junction potentials. Values for Ac-EW-(LSSLLSL)$_3$ (circles) and Ac-RW-(LSSLLSL)$_3$ (squares) are plotted against the base 10 logarithm of the activity ratio. Previously published data for Ac-(LSSLLSL)$_3$ (triangles) are included for comparison.

**Theoretical Analysis of Current-Voltage Curves.** The current-voltage curves in Figure 2 were quantitatively analyzed to determine whether the magnitude of the differences between the conductances of the three peptides were consistent with their N-terminal end charges. This approach has also allowed us to estimate the values of the partial charges at the ends of the α-helix. The curves were analyzed according to an elementary continuum electrodiffusion model in which ions diffuse in a nonlinear electrical field according to eq 2,[12] which was previously employed to describe the Ac-(LSSLLSL)$_3$ channel[11]

$$I(V) = \pi a^2 F \frac{PC[\exp(VF/RT) - 1]}{\int_{-L/2}^{+L/2} \exp[\phi(x,V)F/RT]dx} \qquad (2)$$

in which $I$ is the current, $V$ is the applied voltage, $a$ is the pore radius (estimated as 4 Å for the Ac-(LSSLLSL)$_3$ channel), $F$ is Faraday's constant, $P$ is the sum of cation and anion permeabilities in the pore, $C$ is the electrolyte solution activity, $RT$ is thermal energy, and $L$ is the length of the pore (estimated as 30 Å for the Ac-(LSSLLSL)$_3$ channel). The potential term, $\phi(x,V)$ (eq 3), describes the variation in electrical potential with respect to the displacement ($x$) through the channel as a sum of three contributions:

$$\phi(x,V) = \phi_{app}(x,V) + 180[\phi_{ec}(x) + \phi_{image}(x)] \qquad (3)$$

The center of the channel is taken to be at $x = 0$, and the factor of 180 mV/Å gives $\phi(x,V)$ in mV when $x$, $a$, and $L$ are expressed in Å units. The individual electrical potentials in eq 3 arise from three sources shown diagramatically in Figure 4a. Equation 3a gives the portion of the total variation in the electrical potential with respect to displacement through the channel that is associated with the applied transmembrane voltage:

$$\phi_{app}(x,V) = V(x + L/2)/L \qquad (3a)$$

Equation 3b describes the contribution arising from the channel's end-charges:

$$\phi_{ec}(x) = 6[z_c[a^2 + (x + L/2)^2]^{-0.5} + z_n[a^2 + (x - L/2)^2]^{-0.5}] \qquad (3b)$$

The terms $z_c$ and $z_n$ are the values in electron charge units of each of six noninteracting charges at each of the two ends of the pore ($z_c$ at $x = -L/2$, $z_n$ at $x = +L/2$) arranged radially at a distance of $a = 4$ Å from the cylindrical axis. Equation 3c describes the repulsive potential associated with the ion passing from water into a region bounded by a lower dielectric constant medium (the image charge[13])

$$\phi_{image}(x) = \{f(K)/a - \ln[2/(1 + K)]/KL\} \exp(-x^2/2\sigma^2) \qquad (3c)$$

in which $K = \epsilon_w/\epsilon_p$, $\epsilon_w$ = wall dielectric constant, $\epsilon_p$ = pore dielectric constant, $f(K)$ is a tabulated function[13] describing the dependence of the induced image charge on the dielectric ratio ($K$), and $\sigma$ describes the range of the potential in Å. These parameters were held constant at values found previously to provide excellent fits to the Ac-(LSSLLSL)$_3$ channel's current-voltage curves in 1 M KCl. Those values were $\epsilon_w = 12$ and $\epsilon_p = 80$, giving $f(K) = 1.47$, and $\sigma = 12.4$ Å.[11]

Equation 2 was used to fit each set of current-voltage data in Figure 2. The effective N-terminal charges ($z_n$) and $P$ were the only fitting variables.[14] The computed potentials due to the end charges for each of the three peptides are shown in Figure 4a−c. The determined values of $z_n$ were +0.11, −0.10, and +0.35 for Ac-(LSSLLSL)$_3$, Ac-EW-(LSSLLSL)$_3$, and Ac-RW-(LSSLLSL)$_3$, respectively, while the values of $P$ were nearly identical among the three peptides ($1.4 \pm 0.1 \times 10^{-5}$ cm$^2$/s).

The interpretation of the values of $z_n$ in terms of the actual N-terminal charges requires knowledge of the electrolyte screening factor. Because the two N-terminally charged peptides differ from Ac-(LSSLLSL)$_3$ by the addition of either a negative or positive unit charge to the N-terminus, it is possible to determine both the screening factor and the effective end charge of the parent peptide directly from the experimentally determined values of $z_n$. The effective N-terminal charge $z_n$ on each of the peptides is

$$z_n(\text{Ac-(LSSLLSL)}_3) = S[z_\alpha] = 0.11 \qquad (4)$$

$$z_n(\text{Ac-EW-(LSSLLSL)}_3) = S[z_\alpha - 1] = -0.10 \qquad (5)$$

$$z_n(\text{Ac-RW-(LSSLLSL)}_3) = S[z_\alpha + 1] = 0.35 \qquad (6)$$

in which $S$ is the screening factor, $z_\alpha$ is the partial N-terminal charge arising from the orientation of the amides in the α-helix,

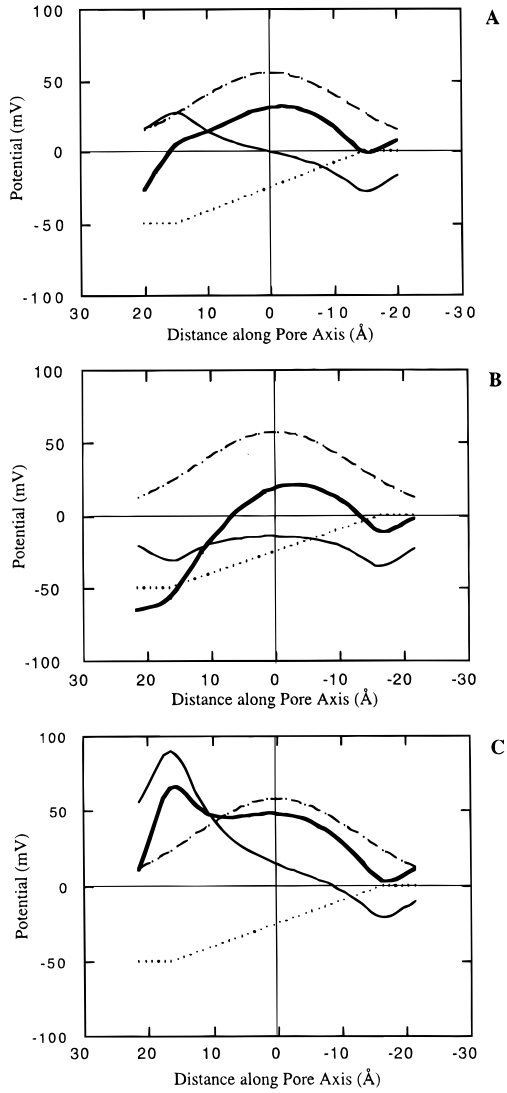


**Figure 4.** Calculated potential profiles for each of the three peptidic ion channels in this study: (A) Ac-(LSSLLSL)$_3$, (B) Ac-EW-(LSSLLSL)$_3$, and (C) Ac-RW-(LSSLLSL)$_3$. Each panel shows the total potential (heavy solid line) for a permeating cation at −50 mV applied transmembrane voltage together with lighter lines showing the isolated contributions of the applied potential (dots), the helix amide end charges (solid), and the repulsive image potential (dashes). The image potential is the same for all ions in each channel, and the other potentials differ only in sign for cations (positive) and anions (negative).

and −1 and +1 in eqs 5 and 6 refer to the unit charge on the N-terminal Glu and Arg residue, respectively. Solution of these eqs gives $S = 0.23 \pm 0.02$ and $z_\alpha = 0.54 \pm 0.02$.

## Discussion

These results show how charged residues near the mouth of an ion channel can significantly affect its ionic conductance. The neutral Ac-(LSSLLSL)$_3$ channel shows a moderate degree of rectification arising from the helical dipole as well as a moderate degree of cation selectivity postulated to arise from the preferential orientation of the Ser side chains within the pore.[6] Formally charged residues can modulate these properties, giving rise to increases or decreases in both rectification and selectivity. In the model channels studied here, the ion flux is largely determined by ion entry rates (the current in these channels is approximately proportional to the electrolyte solution activity between 0.1 and 1 M KCl). Consequently, addition of the N-terminal Glu should increase current due to cations at positive potential and decrease current due to anions at negative potential. Both of these effects contribute to the decreased rectification and increased cation selectivity of this particular channel. The same argument can be applied to deduce the underlying cause of the increased rectification and decreased cation selectivity in the positively charged peptide channel.

The quantitative fitting of data using the electrodiffusion model gave parameters consistent with the physical model. The assumption of a parallel, hexamer bundle of α-helices, together with the total end charge values calculated from the curve fits, yields a value of 0.54 for the effective N-terminal charge of the α-helix, in excellent agreement with accepted values.[8,15,16] The screening factor calculated from these data ($S = 0.23$) indicates somewhat more attenuation of charge effects than would be calculated ($S = 0.36$) from simple Debye−Hückel theory for 1 M ionic strength and a 4 Å distance, but this is hardly surprising given the complexity of the ionic atmosphere near the entrance of the channel.

This electrostatic treatment provides remarkably good agreement with the data, considering the small number of adjustable parameters. Moreover, the fitted values of the parameters are physically quite reasonable, especially the values of the intrinsic partial end charges for the peptide helix. This encourages us to accept the gross features of the structural model involving a parallel bundle of α-helices. However, more detailed theories are clearly required to quantitate the current-voltage curves measured using asymmetric salt solutions.[17] Also, electrostatic theories based on the actual atomic coordinates of the peptide will be needed to further determine whether a six-stranded coiled coil geometry is uniquely consistent with our results or whether five-and/or seven-stranded structures might also account for the data.

The experimental results here, along with their simple interpretation, complement and deepen our understanding of studies involving mutants of large ion channel proteins. Site-directed mutagenesis can help to define which of the many charged residues present in a channel are important for ion permeation. For instance, in the acetylcholine and GABA receptors, site directed mutagenesis has been used to show which of a number of potentially important groups actually influence ion conduction under physiological conditions.[18−20] However, without high resolution structures, it is very difficult to interpret these results in terms of detailed geometric models. The results of the model studies presented here should be relevant to the interpretation of natural ion channel mutation studies. For example, the uncharged channel's cation selectivity suggests a similar bias might be found to underlie the selectivity observed in natural channels. Perhaps this is why the cation selectivity of the acetylcholine receptor is significantly greater than the anion selectivity of the GABA receptor.[21] Also, the large changes in rectification and selectivity we observed due to changing our model peptide's end charges should be magnified under physiological salt concentration (approximately 0.15 M) where the end charges would be less well screened. Thus, our results support and help quantify previous suggestions[22] that end charges play a very important role in modulating the charge selectivity of excitatory and inhibitory receptor ion channels.

(15) Honig, B. H.; Hubbell, W. L.; Flewelling, R. F. *Ann. Rev. Biophysics Biophys. Chem.* **1986**, *15*, 163−193.
(16) Lockhart, D. J.; Kim, P. S. *Science* **1993**, *260*, 198−202.
(17) Chen, D. P.; Lear, J. D.; Eisenberg, R. S. *Biophys. J.* **1997**, *72*, 97−116.
(18) Imoto, K.; Busch, C.; Sakmann, B.; Mishina, M.; Konno, T.; Nakai, J.; Bujo, H.; Mori, Y.; Fukuda, K.; Numa, S. *Nature* **1988**, *335*, 645−648.
(19) Kienker, P.; Tomaselli, G.; Jurman, M.; Yellen, G. *Biophys. J.* **1994**, *66*, 325−334.
(20) Galzi, J.-L.; Devillers-Thiéry, A.; Hussy, N.; Bertrand, S.; Changeux, J.-P.; Bertrand, D. *Nature* **1992**, *359*, 500−505.
(21) Franciolini, F.; Petris, A. *Biochim. Biophys. Acta* **1992**, *1113*, 1−11.
(22) Green, W. N.; Andersen, O. S. *Annu. Rev. Physiol.* **1991**, *53*, 341−359.

## Experimental Section

**General Methods and Material.** All the reactions were carried out under a dry $N_2$ atmosphere. Ethyl acetate, acetonitrile, chloroform ($CHCl_3$), acetic acid, hexane, diethyl ether, anhydrous dichloromethane ($CH_2Cl_2$), anhydrous dimethylformamide (DMF), anhydrous methanol, *N*-hydroxysuccinimide, dicyclohexylcarbodiimide (DCC), diisopropylethylamine (DIEA), acetic anhydride, 10% Pd on activated carbon (Pd/C), pentafluorophenol, 1-(3-dimethylaminopropyl)-3-ethylcarbodiimide hydrochloride (EDC), thioanisole, and the trifluoroacetic acid (TFA) were purchased from Aldrich and used without further purification. Z-Glu(*t*-Bu)-OH and tryptophan were purchased from Advanced ChemTech and used without further purification. Mass determinations were carried out on a VG 70-VSE high-resolution mass spectrometer. Analytical HPLC was performed employing an HP-1090 series system equipped with either a Vydac C18 peptide/protein column (4.6 mm ID $\times$ 25 cm L, 5 $\mu$m) or a Hamilton PRP-1 column (4.1 mm ID $\times$ 25 cm L, 10 $\mu$m). Solvent A was composed of water and 0.1% TFA and, unless stated otherwise solvent B consisted of 90% acetonitrile, 10% water, and 0.1% TFA.

**Peptides.** Ac-(LSSLLSL)$_3$ was prepared as described previously,[11] and Ac-RW-(LSSLLSL)$_3$ was prepared using standard stepwise solid phase methods.[10] Ac-EW-(LSSLLSL)$_3$ was prepared by coupling the preformed dipeptide fragment, Ac-Glu-Trp-OPfp (**4**), to (LSSLLSL)$_3$.

Briefly, the synthesis of **4** begins with coupling tryptophan to Z-Glu(*t*-Bu) via the succinimide ester affording Z-Glu(*t*-Bu)-Trp-OH (**1**) in 96% yield. Hydrogenation of **1** in the presence of acetic anhydride yields Ac-Glu(*t*-Bu)-Trp-OH (**2**) in 77% yield. Ac-Glu(*t*-Bu)-Trp-OPfp (**3**) was synthesized in 58% yield by reacting **2** with pentafluorophenol employing EDC activation. Finally, the *tert*-butyl protecting group of **3** was removed with 10% thioanisole in TFA affording **4** in 57% yield.

**Z-Glu(*t*-Bu)-Trp-OH (1).** A dry 100 mL, round-bottomed flask was charged with Z-Glu(*t*-Bu)-OH (2 g, 5.93 mmol), *N*-hydroxysuccinimide (683 mg, 5.93 mmol), and 12 mL of anhydrous $CH_2Cl_2$. This solution was stirred on an ice bath, and DCC (1.23 g, 5.93 mmol) was added under a blanket of $N_2$. The reaction was stirred for 20 min and then allowed to warm to room temperature and stirred for an additional 4 h. The reaction was filtered to remove the urea byproduct and subsequently evaporated to 1/5 its original volume The reaction solution was then cooled to 4 °C, allowed to sit for 2 h to precipitate the remaining urea byproduct, filtered, and evaporated to yield Z-Glu(*t*-Bu) succinimide ester as a white solid, which was dried under high vacuum. The Z-Glu(*t*-Bu) succinimide ester was then dissolved in 24 mL of anhydrous DMF and tryptophan (1.33 g, 6.52 mmol) was added at once under a blanket of $N_2$. This mixture was stirred on an ice bath, and DIEA (1.03 mL, 5.93 mmol) was added via syringe. After 20 min, the reaction was allowed to warm to room temperature, stirred for an additional 14 h, filtered, transferred to a separatory funnel, and partitioned between 10 mL of 5% HCl and 15 mL of ethyl acetate. The organic phase was collected, and the aqueous phase was extracted with ethyl acetate (1 $\times$ 15 mL). The combined ethyl acetate extracts were washed with 5% HCl (3 $\times$ 10 mL), water (1 $\times$ 10 mL), dried ($Na_2SO_4$), and evaporated to yield an oil which, when evaporated from diethyl ether, yielded 2.97 g (5.67 mmol, 96%) of **1** as a white foam after drying under high vacuum. Mass spectrum (FAB) *m*/*z* 524.2392 [(M + H)$^+$, calcd for $C_{28}H_{34}N_3O_7$, 524.2397]; analytical $C_{18}$ HPLC employing a linear gradient from 20% to 80% solvent B over 30 min, r.t. = 22.0 min.

**Ac-Glu(*t*-Bu)-Trp-OH (2).** A dry 200 mL, round-bottomed flask was charged with **1** (2.75 g, 5.26 mmol), 73 mL of anhydrous methanol, acetic anhydride (0.65 mL, 6.83 mmol), and 10% Pd/C (0.29 g). The $N_2$ atmosphere was replaced with a continuous flow of $H_2$ bubbled through the reaction mixture. After stirring for 3 h, the Pd/C was removed by filtration and washed with warm methanol (2 $\times$ 20 mL). The methanol was evaporated yielding a pink oil which was flash chromatographed on silica ($CHCl_3$/methanol/acetic acid, 8.5:1.5:1) affording 1.75 g (4.05 mmol, 77%) of **2** as a white solid after drying on high vacuum. Mass spectrum (FAB) *m*/*z* 432.2112 [(M + H)$^+$, calcd for $C_{22}H_{30}N_3O_6$, 432.2135]; analytical $C_{18}$ HPLC employing a linear gradient from 20% to 80% solvent B over 30 min, r.t. = 13.8 min.

**Ac-Glu(*t*-Bu)-Trp-OPfp (3).** A dry 50 mL, round-bottomed flask was charged with pentafluorophenol (0.74 g, 4.02 mmol), and then a solution of **2** (1.65 g, 3.82 mmol in 20 mL anhydrous $CH_2Cl_2$) was added via syringe. The solution was stirred on an ice bath and EDC (0.77 g, 4.02 mmol) was added at once under a blanket of $N_2$. The reaction was stirred for 20 min, then allowed to warm to room temperature, stirred for an additional 45 min, transferred to a separatory funnel, washed with 5% HCl (3 $\times$ 15 mL) and water (1 $\times$ 15 mL), and dried ($Na_2SO_4$). The $CH_2Cl_2$ was evaporated affording a yellow solid which was flash chromatographed on silica (ethyl acetate/hexane, 9:1) yielding 1.33 g (2.23 mmol, 58%) of **3** as a yellow solid. Mass spectrum (FAB) *m*/*z* 598.1974 [(M + H)$^+$, calcd for $C_{28}H_{29}N_3O_6F_5$, 598.1977]; analytical $C_{18}$ HPLC employing a linear gradient from 20% to 80% solvent B over 30 min, r.t. = 26.4 min.

**Ac-Glu-Trp-OPfp (4).** A dry 25 mL, round-bottomed flask was charged with **3** (0.5 g, 0.84 mmol), and then 2.7 mL of 10% thioanisole in TFA at 0 °C was added via syringe. The reaction was stirred on an ice bath for 1.5 h after which time, the TFA was evaporated by passing a stream of $N_2$ over the cold solution. The resulting oil was triturated with cold diethyl ether affording 259 mg (0.48 mmol, 57%) of **4** as a light brown solid. Mass spectrum (FAB) *m*/*z* 542.1367 [(M + H)$^+$, calcd for $C_{24}H_{21}N_3O_6F_5$, 542.1351]; analytical $C_{18}$ HPLC employing a linear gradient from 20% to 80% solvent B over 30 min, r.t. = 19.5 min.

**Ac-EW-(LSSLLSL)$_3$-CONH$_2$.** A dry vial was charged with $H_2N$-(LSSLLSL)$_3$-$CONH_2$ (8.0 mg, 3.7 $\mu$ mol), **4** (6.0 mg, 11.1 $\mu$ mol), and 140 $\mu$L of anhydrous DMF. The solution was stirred on an ice bath and DIEA (0.7 $\mu$L, 4.07 $\mu$mol) was added via syringe. The reaction was stirred for 1 h, then allowed to warm to room temperature, and stirred for an additional 4 h after at which time cold diethyl ether was added to the solution resulting in the formation of a precipitate. The solid was collected by filtration and purified by analytical PRP-1 HPLC employing isocratic conditions of 80% B (solvent B is composed of 60% acetonitrile, 30% isopropyl alcohol, 10% water, and 0.1% TFA). The yield as determined by HPLC was nearly quantitative; a small sample (200 $\mu$g) was purified for ion channel measurements. Mass spectrum (ESI) 2513.6 [(M + H)$^+$, calcd 2514.4].

**Fluorescence Measurements.** The peptide's tryptophan emission spectrum was determined using a Spex Fluorolog instrument. Excitation was at 280 nm in 1 cm quartz cells. Spectra were determined at 5 $\mu$M peptide concentration in pH 7.6, 10 mM phosphate buffer containing POPC lipid vesicles at 150 $\mu$M. The emission spectrum, corrected for instrument wavelength response and buffer plus vesicle scattering background, showed a maximum at 332 nm, consistent with the Trp being located in a moderately apolar environment on the hydrophobic face of a membrane-associated peptide $\alpha$-helix.[10]

**Ion Channel Measurements.** Peptides were incorporated from methanolic solutions into diphytanoyl phosphatidylcholine planar bilayers and single channel current-voltage (I-V) curves were determined as previously described.[5] The electrolyte contained 1 M KCl, 0.2 mM EDTA, and 5 mM HEPES at pH 7.2 (Ac-(LSSLLSL)$_3$, Ac-RW-(LSSLLSL)$_3$), or 25 mM CHES at pH 9.2 (Ac-EW-(LSSLLSL)$_3$).[9] Data points for current-voltage curves were determined by averaging baseline-subtracted currents measured using 10 V/s voltage ramps triggered by single channel openings. Only channels whose current (at the negative holding voltage) lay within the dominant open current histogram peak were used for averaging. At least 20 ramps were averaged for each peptide. Data (weighted using standard deviations of currents at each voltage point) were fit using the program MLAB (Civilized Software, Bethesda MD) to a previously described fitting function[11] based on a parallel hexamer bundle model of the channel with ion permeation described by a mean-potential electrodiffusion model[12] and parameters determined as described in the Results section. Potentials measured in asymmetric solutions were corrected for liquid junction potentials as described previously.[5] No corrections for osmotic pressure differences were made because previous measurements for the Ac-(LSSLLSL)$_3$ channel[5] showed this effect to be negligible.

**Acknowledgment.** This work was supported by the United States Office of Naval Research.

JA9629672